Polymers Grafted to Convex Surfaces: A Variational Approach

Hao Li* and Thomas A. Witten

The James Franck Institute, The University of Chicago, Chicago, Illinois 60637

*Received July 9, 1993; Revised Manuscript Received October 29, 1993**

ABSTRACT: We study the asymptotic static properties of long polymers grafted to a convex surface in a solvent using a variational approach. The equilibrium state is obtained by minimizing the free energy with respect to the free end distribution and the stretching profiles of the polymers. We simplify the minimization by assuming that the stretching profiles of all the chains are the same up to an overall scale factor. This approach when applied to a planar surface reproduces results identical to those obtained by Milner, Witten, and Cates using a self-consistent field approach. For polymers grafted to a cylinder or a sphere, we find two distinct regions: an exclusion zone ($r < r_c$) and an end distributed region ($r_c < r < h^*$). The monomer density profile $n(r)$ in the exclusion zone is found to be consistent with the scaling results based on a blob picture. In the end distributed region, $n(r)$ is a concave down function and vanishes continuously at the top of the grafting layer. Independently, we found the exact self-consistent solutions for a cylindrical brush in the strong curvature limit, by solving the integral equations of Ball, Marko, Milner, and Witten using the Wiener–Hopf technique. Our simple variational approach produces qualitatively correct features of this exact solution.

I. Introduction

In this paper, we investigate the static properties of long polymers grafted to convex surfaces in contact with a solvent. Such a problem arises naturally in many physical systems; among the examples are star and comb polymers with many arms, colloidal suspensions stabilized by grafting polymers to the surfaces of the particles, and diblock copolymer micelles formed by segregation of immiscible chains. Understanding the static behavior of a single unit is a necessary step toward unraveling other properties of interest such as forces between colloidal particles, micromorphologies of copolymers, etc.

Previous studies on end-confined polymers have revealed qualitative differences between these and unattached polymers.[1] de Gennes[2] and Alexander[3] first accounted for the strong elongation of end-confined (grafted) polymers and the associated internal pressure at the level of scaling laws. Helfand and Wasserman invented a self-consistent-field method to determine the chain conformations and the pressure profile explicitly.[4] Several generalizations and numerical implementations have since been developed.[5–8] More recently Semenov[9] and Milner, Witten, and Cates[10] simplified the SCF theory in the asymptotic limit of long chains and strong elongation. A similar approach has been developed by Zhulina and coworkers.[11] The central findings of the theory were that the monomer density away from the grafting surface is parabolic, and free ends are distributed throughout the layer. For polymers grafted to the outside of a cylinder or a sphere, quite different behavior was found. The effect of this convex curvature was studied by Ball, Marko, Milner, and Witten[12] who extended the asymptotic SCF approach to convex surfaces and solved exactly the problem of cylindrical brush under melt conditions. They found that free ends are excluded from a zone near the surface to avoid overfilling the space, and the pressure profile is no longer parabolic (as anticipated by Semenov[9]). In the same paper, Ball et al. also showed quite generally how one can cast the self-consistent conditions into integral equations.

In this paper, we develop a general variational approach to study curved brushes in contact with solvent. The equilibrium properties are obtained by minimizing the free energy with respect to all the possible trajectories of polymer chains. The free energy is expressed using a SCF approach. Also, like refs 9 and 10, we assume that each chain with a given free-end position has a single stretching profile where fluctuations around the ground state are ignored. These are legitimate for high grafting density where chains are strongly stretched.[9] We shall show that by making some simple and reasonable ansatz about the stretching profiles of the polymers, the problem can be drastically simplified and yet many interesting features can be revealed. The variational solution can be systematically improved by searching for the free energy minimum in a larger and larger configuration space. In the limiting case where the grafting surface is flat, we find results identical to those obtained by Milner, Witten, and Cates using the SCF approach.[10] For polymers grafted to a convex sphere or cylinder, we found two distinct regions: (i) The region $r < r_c$ is an exclusion zone with no free ends. The monomer density profile $n(r)$ in this region is consistent with the scaling results based on a blob picture.[13,14] (ii) Beyond the exclusion zone is an end distributed region ($r_c < r < h^*$) where $n(r)$ is a concave down function and vanishes continuously at the top of the grafting layer $r = h^*$. The exclusion zone radius r_c is a specific fraction of the height h^* in the strong curvature limit. As an alternative method and a check for the variational results, we solved exactly the self-consistent integral equations[12] for a cylindrical brush in a solvent, in the strong curvature limit. We obtained the density profile, free end distribution, and free energy in closed form. We found that addition of solvent makes the exclusion zone smaller ($r_c/h^* = 4/(3\pi)$) compared with the melt case ($r_c/h^* = 2/\pi$). Our simple variational approach produces the same qualitative features as this exact solution.

The paper is organized as follows. In section II, after a general description of the variational principle, we apply it to polymers grafted to various surfaces: plane, sphere, and cylinder. We show how the results can be improved systematically by using a better and better ansatz for the stretching profiles. In section III, we first briefly sketch the key ideas that lead to the self-consistent integral equations for a cylindrical brush in a solvent. We then present our exact solution of the integral equations in the strong curvature limit. Various quantities are calculated in closed form. Section IV contains a discussion of results

* Abstract published in *Advance ACS Abstracts*, December 15, 1993.

0024-9297/94/2227-0449$04.50/0

obtained in sections II and III and possible extensions of our approach.

II. Variational Approach

In this section, we develop a general variational approach and apply it to polymers grafted to various surfaces.

2.1. Theoretical Description. To begin with, we specify the trajectories of polymers by $\mathbf{r}_i(t)$, the position of the tth monomer in the ith chain. We shall adopt a continuous descripton of the polymers suitable for long, flexible chains. In order to focus on the effects of stretching and convex curvature, we choose to simplify our treatment of the solvent. We treat the "marginal solvent" regime, in which two-body excluded volume effects are weak so that the local Flory swelling of the chains can be ignored on a scale larger than the interchain distance. Semidilute chains in such a "marginal" solvent are Gaussian at all length scales due to screening, but they are dilute enough such that three-body and higher-order interactions are negligible. In a marginal solution of free polymers the Edwards RPA description of the chain statistics is applicable.[15] The scaling properties of a marginal solvent are somewhat different from those of ordinary good solvents. These differences are reflected in some of our results for grafted chains. The free energy of grafted polymers in a marginal solvent can be expressed as

$$\mathcal{F} = \sum_i \int_0^N \frac{1}{2a^2}\left(\frac{d\mathbf{r}_i(t)}{dt}\right)^2 dt + \frac{\nu}{2}\int n^2(\mathbf{r})\, d^3V \quad (2.1)$$

where the first term represents the elastic energy of stretching of the polymers which is entropic in origin, and the second term is the excluded-volume interaction between polymers. Here a is a microscopic length, ν an interaction parameter characterizing the quality of the solvent, and N the total number of monomers in one chain. The monomer density $n(\mathbf{r})$ is related to trajectories via

$$n(\mathbf{r}) = \sum_i \int \delta(\mathbf{r} - \mathbf{r}_i(t))\, dt \quad (2.2)$$

The equilibrium properties are determined by the partition function,

$$Z = \sum_{\{\mathbf{r}_i(t)\}} \exp(-\mathcal{F}[\{\mathbf{r}_i(t)\}]) \quad (2.3)$$

where the summation is to be carried out for all the possible trajectories. For brushes with high grafting density, chains are strongly stretched. The fluctuations become unimportant.[9] The task is then reduced to finding the optimal $\mathbf{r}_i(t)$ that minimize the free energy $\mathcal{F}[\{\mathbf{r}_i(t)\}]$. We shall show that by restricting the search in a subspace of $\{\mathbf{r}_i(t)\}$, the problem of minimization can be drastically simplified.

2.2. Polymers Grafted to a Flat Surface. Consider polymers with one end grafted to a plane $(x, y, 0)$. Due to the translational invariance parallel to the plane, we may consider only the stretch in the z direction and classify the trajectories $\mathbf{r}_i(t)$ by $z(z_0, t)$, with z_0 the free end position. In the strong stretching regime, backward motion of the chains will be ignored, hence $z(z_0, t)$ increases monotonically from 0 to z_0 as t varies from 0 to N. Let $\rho(z_0)\, dz_0$ be the number of free ends per unit area in the interval $z_0 - z_0 + dz_0$, the monomer density $n(z)$ can be expressed as

$$n(z) = \int_z^h \frac{dt\ (z, z_0)}{dz}\rho(z_0)\, dz_0 \quad (2.4)$$

where $t = t(z, z_0)$ is the inverse function of $z = z(z_0, t)$. The free energy of the system from eq 2.1 is

$$\mathcal{F} = \int_0^h dz_0\, \rho(z_0) \int_0^N \frac{1}{2a^2}\left(\frac{dz\ (z_0, t)}{dt}\right)^2 dt + \frac{\nu}{2}\int_0^h n^2(z_0)\, dz_0 \quad (2.5)$$

The variational problem is to find the minimum of the above free energy in the space of all possible functions $z(z_0, t)$ and $\rho(z_0)$, subject to the constraint of the total number of monomers,

$$\int_0^h n(z_0)\, dz_0 = N\sigma \quad (2.6)$$

where σ is the number of grafted chains per unit area. We shall show in the following how one can get better and better solutions using improved trial functions for $z(z_0, t)$ and $\rho(z_0)$.

(i) Alexander–de Gennes Approximation. This approximation assumes that all the chains stretch uniformly to a height h. Hence $\rho(z_0) = \sigma\delta(z_0 - h)$, $z(h, t) = ht/N$, and

$$\mathcal{F} = \frac{\sigma h^2}{2a^2 N} + \nu\sigma^2\frac{N^2}{2h} \quad (2.7)$$

where σ is the number of grafted chains per unit area. Minimizing the above free energy with respect to h leads to

$$h^* = (\nu\sigma a^2/2)^{1/3}N \quad (2.8)$$

and

$$\mathcal{F}_{\min} = (27/32)^{1/3}(\nu^2\sigma^5/a^2)^{1/3}N \quad (2.9)$$

(ii) Relaxing the Constraint for the Free Ends. As an improvement to Alexander–de Gennes approximation, we relax the δ function constraint for the free ends while still using the uniform stretching profile $z(z_0, t) = z_0 t/N$. With a general distribution $\rho(z_0)$, eq 2.4 becomes $n(z) = \int_z^h \rho(z_0)\, dz_0 N/z_0$. This is inverted to give $\rho(z) = (-z/N)\, \partial n(z)/\partial z$, and the free energy

$$\mathcal{F}[n(z)] = \int_0^h \left[-\frac{z^3}{2a^2N^2}\frac{\partial n(z)}{\partial z} + \frac{\nu}{2}n^2(z) + \alpha n(z)\right] dz \quad (2.10)$$

where α is a Lagrange multiplier which takes care of the total-number-of-monomers constraint. The optimal $n(z)$ is given by the Euler–Lagrange equation

$$\frac{\partial}{\partial z}\frac{\delta\mathcal{F}}{\delta\partial n(z)/\partial z} - \frac{\delta\mathcal{F}}{\delta n(z)} = 0 \quad (2.11)$$

which yields

$$n(z) = \frac{-\alpha}{\nu} - \frac{3z^2}{2\nu a^2 N^2} \quad (2.12)$$

and

$$\rho(z) = \frac{3}{\nu a^2 N^3}z^2 \quad (2.13)$$

In this simple approximation the monomer density profile is parabolic, and free ends are distributed throughout the layer.

The layer height h^* and constant α can be fixed by using eq 2.6 and requiring $n(h^*) = 0$.[16] We find

$$h^* = (\nu\sigma a^2)^{1/3}N \quad (2.14)$$

$$\mathcal{F}_{\min} = 9/10(\nu^2\sigma^5/a^2)^{1/3}N \quad (2.15)$$

This height is 1.26 times larger than that of the Alexander–de Gennes brush, while the energy is 0.95 times as large. This demonstrates that Alexander–de Gennes' solution is unstable against smearing of the free ends. Within the uniform stretching ansatz, it is energetically favorable to smear the free ends all over the grafting layer and make the density profile a parabola. Although not exact, this solution already has all the qualitatively correct features of the exact solution.

(iii) General Stretching. To improve the results further, we consider general stretching $z(z_0, t)$. We shall assume that the stretching profiles of all the chains are the same up to an overall scale factor, namely

$$z(z_0, t) = z_0 f(t) \tag{2.16}$$

where $f(t)$ is a monotonically increasing function satisfying $f(t) = 0$ and $f(1) = 1$. With this ansatz, the configuration space is restricted to two functions $\rho(z_0)$ and $f(t)$ which we will find by minimizing the free energy. After some algebra, the relation between $\rho(z)$ and $n(z)$ from eq 2.4 can be written as

$$n(z) = \int_0^N \rho\left(\frac{z}{f(t)}\right)\frac{dt}{f(t)} \tag{2.17}$$

For a general $f(t)$, the above equation cannot be inverted explicitly. We choose to implement the constraint using Lagrange multipliers $\beta(z)$. This leads to a free energy for variation

$$\mathcal{F} = \int_0^h dz\, \rho(z)\frac{z^2}{2a^2}\int_0^N \left(\frac{df}{dt}\right)^2 dt + \int_0^h \frac{\nu}{2} n^2(z)\, dz + \int_0^h \beta(z)\left[n(z) - \int_0^N \rho\left(\frac{z}{f(t)}\right)\frac{dt}{f(t)}\right] dz + \alpha\int_0^h n(z)\, dz \tag{2.18}$$

Minimizing the above free energy yields the following equations

$$\frac{\delta\mathcal{F}}{\delta\rho(z)} = \frac{z^2}{2a^2}\int_0^N (df/dt)^2\, dt - \int_0^N \beta(zf(t))\, dt = 0 \tag{2.19a}$$

$$\frac{\delta\mathcal{F}}{\delta n(z)} = \nu n(z) + \beta(z) + \alpha = 0 \tag{2.19b}$$

$$\frac{d}{dt}\frac{\delta\mathcal{F}}{\delta df/dt} - \frac{\delta\mathcal{F}}{\delta f} = \frac{d^2 f}{dt^2}\int_0^h \frac{z^2}{a^2}\rho(z)\, dz - \int_0^h \frac{\beta(zf(t))}{f(t)}[z\rho'(z) + \rho(z)]\, dz = 0 \tag{2.19c}$$

$$\frac{\delta\mathcal{F}}{\delta\beta(z)} = n(z) - \int_0^N \rho(z/f(t))\frac{dt}{f(t)} = 0 \tag{2.19d}$$

The above equations can be solved by employing the following observations. Suppose we expand $\beta(x)$ in its Taylor series. Since eq 2.19a is true for arbitrary z, and $f(t)$ increases from 0 to 1 as t goes from 0 to N, we conclude that only the term quadratic in x is nonvanishing, i.e., $\beta(x) = cx^2$. This implies through eq 2.19b that $n(z)$ is parabolic. Substituting $\beta(x)$ into eq 2.19c yields

$$\frac{1}{2a^2}\frac{d^2 f}{dt^2} + cf(t) = 0 \tag{2.20}$$

which together with the conditions $f(t) = 0$ and $f(N) = 1$ gives

$$f(t) = \frac{\sin\sqrt{2ca}t}{\sin\sqrt{2ca}N} \tag{2.21}$$

Finally, the constant c is fixed by substituting $f(t)$ back into eq 2.19a. We find $c = \pi^2/(8a^2N^2)$ so

$$n(z) = -\frac{\alpha}{\nu} - \frac{\pi^2}{8\nu a^2 N^2}z^2 \tag{2.22}$$

and

$$f(t) = \sin\frac{\pi}{2N}t \tag{2.23}$$

The equilibrium height h^* and free energy can be calculated using the conservation of total number of monomers and the condition $n(h^*) = 0$. The results are

$$h^* = \left(\frac{12}{\pi^2}\right)^{1/3}(\sigma\nu a^2)^{1/3}N \tag{2.24}$$

and

$$\mathcal{F}_{\min} = \frac{9}{10}\left(\frac{\pi^2}{12}\right)^{1/3}(\sigma^5\nu^2/a^2)^{1/3}N \tag{2.25}$$

These are exactly the same results obtained by Miller, Witten, and Cates[10] in the SCF approach. Equation 2.23 implies that there is no stretching at the free ends, which comes out naturally from the variation.

2.3. Polymers Grafted to a Sphere. The variational approach can be easily extended to a spherical brush. Here we consider the limit where the height of the grafting layer h is much larger than the radius of the grafting surface (e.g., star polymers). Due to the rotational symmetry, we need only to consider radial stretching of the polymers. Denote $r(r_0, t)$ the trajectory with the free end at r_0 and $\rho(r_0)$ the free end density per unit volume. Due to the geometric constraint, the space available is rapidly decreasing as the grafting center is approached. To avoid overfilling the space, free ends must be excluded from an inner region $0 < r < r_c$, as first pointed out by Semenov.[9] Anticipating such an exclusion zone, the density $n(r)$ is related to $\rho(r)$ and trajectories through

$$n(r) = \int_{\mathrm{Max}[r,r_c]}^h \left(\frac{r_0}{r}\right)^2 \rho(r_0)\frac{dt(r, r_0)}{dr}\, dr_0 \tag{2.26}$$

The free energy of the system is

$$\mathcal{F} = \int_{r_c}^h 4\pi r_0^2 \rho(r_0)\, dr_0 \int_0^N \frac{1}{2a^2}\left(\frac{dr(r_0, t)}{dt}\right)^2 dt + \frac{\nu}{2}\int_0^h n^2(r)\, 4\pi r^2\, dr \tag{2.27}$$

Similar to the planar brush case, we need to find $\rho(r_0)$ and $r(r_0, t)$ that minimize $\mathcal{F}$.

(i) Delta Function End Distribution. To extend the Alexander–de Gennes approximation to a spherical brush, we assume that all the chains stretch up to the same height h, i.e., $\rho(r) = f\delta(r - h)/(4\pi h^2)$, where f is the total number of grafted chains (number of arms for a star polymer). The free energy depends on a single trajectory $r(t)$,

$$\mathcal{F} = \int_0^N \frac{f}{2a^2}\left(\frac{dr}{dt}\right)^2 dt + \frac{\nu}{2}\int_0^h \left(\frac{f\, dt}{4\pi r^2\, dr}\right)^2 4\pi r^2\, dr \tag{2.28}$$

In terms of $v(r) \equiv dr/dt$, the free energy for variation can be written as

$$\mathcal{F} = \int_0^h dr\left[\frac{fv(r)}{2a^2} + \frac{\nu f^2}{8\pi r^2 v(r)^2} + \frac{\lambda}{v(r)}\right] \tag{2.29}$$

with λ a Lagrange multiplier which takes care of the

monomer number constraint

$$\int_0^h \frac{dr}{v(r)} = N \tag{2.30}$$

Variation with respect to $v(r)$ leads to the following equation:

$$\frac{v(r)^2}{2a^2} - \frac{\nu f}{4\pi r^2 v(r)} = \frac{\lambda}{f} \tag{2.31}$$

For a given h, eqs 2.30 and 2.31 determine $v(r)$ and the corresponding free energy $\mathcal{F}[h]$. The equilibrium height h^* is obtained by minimizing $\mathcal{F}[h]$. The exact solution will be presented in the Appendix. Here for simplicity we seek an approximate solution with a simple form which will be used next for the variational calculation with end constraint relaxed. Since most of the stretching energy is distributed in the region $r \ll h$ where the repulsion between chains is strong, the approximate solution we are seeking must capture the correct small r behavior. From eq 2.31, we see that $v(r) \sim (a^2\nu f)^{1/3} r^{-2/3}$ for small r or $r(t) \sim (a^2\nu f)^{1/5} t^{3/5}$ for small t. This leads to $n(r) \sim (f^2 a^{-2} \nu^{-1})^{1/3} r^{-4/3}$, which is the same scaling obtained by Daoud and Cotton[13] based on a blob picture. As an approximate solution, we assume such a scaling extends throughout the layer, i.e., $r(t) = h(t/N)^{3/5}$, and minimize the free energy in eq 2.28 by varying h. The results are

$$h^* = \left(\frac{125}{72\pi}\right)^{1/5} (\nu f a^2 N^3)^{1/5} \tag{2.32}$$

$$\mathcal{F}_{\min} = \frac{3}{2}\left(\frac{125}{72\pi}\right)^{2/5}\left(\frac{f^7 \nu^2 N}{a^6}\right)^{1/5} \tag{2.33}$$

This scaling with N, f, and ν agrees with simple Flory estimates. The scaling of h^* (but not $\mathcal{F}_{\min}$) also agrees with that predicted for good solvents by Daoud and Cotton.[13] Daoud and Cotton predict $h^* \sim f^{(1-\tilde{\nu})/2} N^{\tilde{\nu}}$, where $\tilde{\nu}$ is the swelling exponent. This agrees with eq 2.32 if one uses the nearly exact Flory value $\tilde{\nu}_F = {}^3/_5$. The variational method also gives an estimate for the coefficients, which cannot be obtained by simple scaling arguments.

(ii) Relaxing the End Constraint. In analogy to the planar brush case, we improve the solution in (i) by relaxing the δ function constraint for the free ends. Consider a general distribution $\rho(r_0)$ in a region $r_c < r < h$. We assume that all the chains have similar power law stretching,

$$r(r_0, t) = r_0 (t/N)^{3/5} \tag{2.34}$$

Our strategy is first to find the optimal distribution for a given r_c and h and the corresponding free energy $\mathcal{F}[h, r_c]$. We then determine the equilibrium h^* and r_c by minimizing $\mathcal{F}[h, r_c]$.

Using the ansatz eq 2.34, eq 2.26 becomes

$$n(r) = \frac{5N}{3} r^{-4/3} \int_{\mathrm{Max}[r,r_c]}^h \rho(r_0) r_0^{1/3}\, dr_0 \tag{2.35}$$

which can be inverted to give $\rho(r_0)$ in terms of $n(r)$ in the end distributed region $r_c < r < h$,

$$\rho(r) = -\frac{3}{5N} r^{-1/3} \frac{\partial}{\partial r}[n(r) r^{4/3}] \tag{2.36}$$

Equation 2.35 also determines the monomer density in the exclusion zone by its value at the boundary

$$n(r) = \left(\frac{r}{r_c}\right)^{-4/3} n_-(r_c) \qquad r < r_c \tag{2.37}$$

with $n_-(r_c) = n(r \to r_c^-)$. Equations 2.36 and 2.37 enable us to express the free energy in terms of $n_-(r_c)$ and $n(r)$ in the region $r_c < r < h$. The distinction between $n_-(r_c)$ and $n_+(r_c)$ is necessary since in general we should allow a discontinuity of $n(r)$ to explore all possible configurations. Such a discontinuity corresponds to a δ function in the free end density at the boundary. To exclude unphysical states, we must have $n_-(r_c) \geq n_+(r_c)$ (no negative free ends). Similarly, a jump at h should satisfy $n(h_-) \geq n(h^+) = 0$. Using eqs 2.36 and 2.37, the total free energy (from eq 2.27) for variation is

$$\mathcal{F} = 4\pi B \int_{r_c^-}^{h^+} dr_0 \left[-2r_0^4 n(r_0) - \frac{3}{2} r_0^5 \frac{\partial n}{\partial r}\right] + 6\pi\nu r_c^3 n_-^2(r_c) + \frac{\nu}{2}\int_{r_c}^h n^2(r) 4\pi r^2\, dr + \alpha\left[\frac{12}{5}\pi r_c^3 n_-(r_c) + \int_{r_c}^h 4\pi r^2 n(r)\, dr\right] \tag{2.38}$$

with $B = 9/(25N^2a^2)$. The first term in the above equation is the stretching energy. The integration is from r_c^- to h^+ in order to include the contributions from possible δ function end density at r_c or at h. Variation with respect to $n(r)$ and $n_-(r_c)$ gives

$$n(r) = -\frac{\alpha}{\nu} - \frac{11B}{2\nu} r^2 \qquad h > r > r_c$$
$$n_-(r_c) = -\frac{\alpha}{5\nu} - \frac{11B}{2\nu} r_c^2 \tag{2.39}$$

From the above equations, we see that the monomer density profile in the end distributed region is parabolic. We speculate that this is general as long as the assumption $r(r_0, t) = r_0 f(t)$ is made, regardless of the specific choice for $f(t)$. For a given r_c and h, eqs 2.37 and 2.39 enable us to solve for α through conservation of the total number of monomers, and the free energy is obtained by substituting eq 2.39 back into eq 2.38 (without the α term). The resulting free energy $\mathcal{F}[h, r_c]$ is a rational function of h and r_c. Notice that for general h and r_c, the density profile calculated from eq 2.39 will be discontinuous at r_c and h.

Minimizing $\mathcal{F}[h, r_c]$ determines optimal h and r_c. The search is restricted in the physical region defined by $n_-(r_c) \geq n_+(r_c)$, $n_-(h) \geq 0$. We find that the smooth profile ($n(r)$ is continuous at r_c and h) has the lowest energy. There is an exclusion zone proportional to the layer height h^*,

$$r_c/h^* = 0.938\,083 \tag{2.40}$$

with

$$h^* = 0.914343(fN^3a^2\nu)^{1/5} \tag{2.41}$$

The corresponding free energy is

$$\mathcal{F}_{\min} = 1.18237(f^7\nu^2 N/a^6)^{1/5} \tag{2.42}$$

which is about 0.1% lower than the free energy with end constraint (eq 2.33). The monomer density and free end density are

$$n(r) = \begin{cases} \frac{11B}{2\nu}(h^{*2} - r^2) & h^* > r > r_c \\ \left(\frac{r}{r_c}\right)^{-4/3} n(r_c) & r < r_c \end{cases} \tag{2.43}$$

and

$$\rho(r) = \begin{cases} \frac{11B}{5N\nu}(5r^2 - 2h^{*2}) & h^* > r > r_c \\ 0 & r < r_c \end{cases} \tag{2.44}$$

From eq 2.43, we see that $n(r)$ is concave up in the exclusion zone, concave down in the end distributed region, and vanishes smoothly at the top of the layer. We expect that such a smooth profile will lead to softer interaction than

the Daoud and Cotton star when weakly compressed. In fact, we find

$$\frac{\partial^2\mathcal{F}}{\partial^2 h} = \frac{\partial^2\mathcal{F}}{\partial^2 r_c} = \frac{\partial^2\mathcal{F}}{\partial h \partial r_c}\bigg|_{h^*,r_c^*} = 0 \tag{2.45}$$

This implies for a symmetric compression, $\delta\mathcal{F} \propto \delta h^3$, in contrast to $\delta\mathcal{F} \propto \delta h^2$ for the Daoud and Cotton star. We expect that this is also true for nonsymmetric compression which is more physically relevant.

2.4. Polymers Grafted to a Cylinder. As a consistency check, we apply the method developed in section 2.2 to a strongly curved cylindrical brush (e.g., comb polymers) in order to compare with the exact solution in section III. All the calculations are parallel to the spherical case. With a δ function end distribution, similar calculation gives $r(t) \sim (a^2\nu\epsilon)^{1/4}t^{3/4}$, $n(r) \sim (a^{-2}\nu^{-1}\epsilon^2)^{1/3}r^{-2/3}$. The layer height and free energy are

$$h^* = \left(\frac{32}{27\pi}\right)^{1/4}(\nu\epsilon a^2 N^3)^{1/4} \tag{2.46}$$

$$\mathcal{F}_{min} = \sqrt{\frac{3}{2\pi}}(\nu\epsilon^3 a^{-2}N)^{1/2} \tag{2.47}$$

where ϵ is the number of grafted chains per unit length.

For general end distribution, the ansatz we made for the trajectories is $r(r_0, t) = r_0(t/N)^{3/4}$. Again we find the lowest energy configuration has a smooth density profile. A finite exclusion zone is found with

$$r_c/h^* = 0.790\,569 \tag{2.48}$$

and

$$h^* = 0.855857(N^3a^2\nu\epsilon)^{1/4} \tag{2.49}$$

The density profile is similar to that of a spherical brush but has a different scaling in the exclusion zone

$$n(r) = \begin{cases} \frac{10D}{\nu}(h^{*2} - r^2) & h^* > r > r_c \\ \left(\frac{r}{r_c}\right)^{-2/3} n(r_c) & r < r_c \end{cases} \tag{2.50}$$

with $D = 9/(64N^2a^2)$. The free end density is given by

$$\rho(r) = \begin{cases} \frac{5D}{N\nu}(4r^2 - h^{*2}) & h^* > r > r_c \\ 0 & r < r_c \end{cases} \tag{2.51}$$

These results are plotted in Figure 1 (dotted lines) to compare with the results from the exact self-consistent solution (presented in the next section). Using eqs 2.50 and 2.51, the free energy is calculated as

$$\mathcal{F}_{min} = 0.68671(\nu\epsilon^3 N/a^2)^{1/2} \tag{2.52}$$

which is about 1% lower than the one with end constraint (eq 2.47).

III. Exact Solution for a Cylindrical Brush in the Strong Curvature Limit

In this section, we analyze cylindrical brush in a solvent using the SCF approach previously developed by Milner, Witten, and Cates.[10] Our analysis is based on self-consistent integral equations previously derived by Ball, Marko, Milner, and Witten.[12] In the strong curvature limit, we solved the integral equations exactly and obtained various quantities in closed form. To be self-contained, we shall first briefly sketch the derivation of the integral equations in section 3.1. The results from the exact solution will be presented in section 3.2.

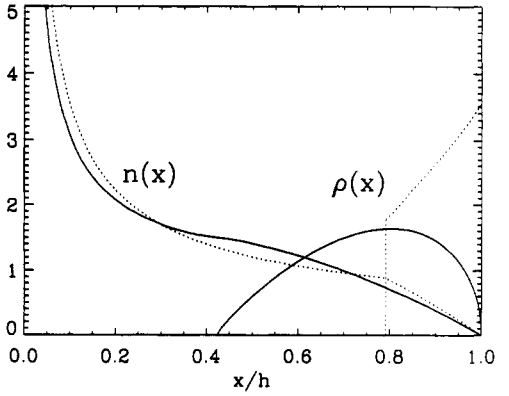

Figure 1. Monomer density ($n(x)$) and free end density ($\rho(x)$) as functions of distance from the grafting center (normalized by the layer height h) for a cylindrical brush in a solvent in the strong curvature limit, from the exact self-consistent solution (solid lines) and the variational calculation (dotted lines). The results are normalized by the corresponding average value $\bar{n} = N\epsilon/(\pi h^{*2})$ and $\bar{\rho} = \epsilon/(\pi h^{*2})$.

3.1. Self-Consistent Field Approach. In the SCF approach, the effect of the excluded volume interaction between polymer chains is considered as a mean potential field which needs to be determined self-consistently. This is similar in spirit to the Hartree–Fock approximation in dealing with many-electron systems. Due to the potential field, the free energy increase by adding the ith chain to the system is

$$S = \int_0^N \frac{1}{2a^2}\left(\frac{d\mathbf{r}_i(t)}{dt}\right)^2 dt + \int_0^N \mu(\mathbf{r}_i(t))\,dt \tag{3.1}$$

Here $\mu(\mathbf{r})$ can be interpreted as work required to insert a monomer at $\mathbf{r}$. In a marginal solvent, $\mu(\mathbf{r}) = \nu n(\mathbf{r})$. The mechanical balance of the chain is achieved when $\mathbf{r}_i(t)$ minimizes the action S. This can be viewed as a particle moving in a potential $-\mu(\mathbf{r})$. The potential $\mu(\mathbf{r})$ must be subject to a number of constraints. Since there is no stretching at the free end, the particle starts at zero velocity. We call $T(\mathbf{r})$ the time it takes for a particle to fall to the grafting surface starting at $\mathbf{r}$ with zero initial velocity. The fact that the total number of monomers N is fixed implies that $\mu(\mathbf{r})$ should be such that for any $\mathbf{r}$ where free ends can be found, $T(\mathbf{r}) = N$. This is the *equal time* constraint. Furthermore, once $\mu(\mathbf{r})$ is given, the trajectories $\mathbf{r}_i(t)$ are determined, which in turn determines $n(\mathbf{r})$ through eq 2.2. $n(\mathbf{r})$ determined this way should be *self-consistent*.

For a cylindrical brush, the equal time and self-consistent constraints can be expressed explicitly to yield a pair of integral equations. Due to rotational symmetry, only radial motion needs to be considered. Using variable $x = r - R$ (R is the radius of the grafting surface), the conservation of energy yields

$$\frac{1}{2a^2}\left(\frac{dx}{dt}\right)^2 - \mu(x) = -\mu(x_0) \tag{3.2}$$

which can be used to calculate the falling time $T(x_0)$ as

$$T(x_0) = -\int_{x_0}^0 dx \frac{1}{\sqrt{2}a}[\mu(x) - \mu(x_0)]^{-1/2} \tag{3.3}$$

It is convenient to write eq 3.3 in terms of variable μ (since μ is a monotonically decreasing function of x),

$$T(\mu_0) = -\frac{1}{\sqrt{2}a}\int_{\mu_0}^P d\mu \frac{dx}{d\mu}[\mu - \mu_0]^{-1/2} \tag{3.4}$$

where P is the potential at the surface. Anticipating an exclusion zone $0 < x < x_c$, we expect $T(\mu) = N$ for $\mu < \mu(x_c)$

$\equiv Q$. Then eq 3.4 can be inverted to give

$$\left.\frac{dx}{d\mu}\right|_{\mu_0} = \frac{\sqrt{2}a}{\pi}\int_{\mathrm{Max}(\mu_0,Q)}^{P} d\mu \frac{dT}{d\mu}[\mu - \mu_0]^{-1/2} \quad (3.5)$$

where the equal time constraint is explicitly included in the lower limit of the integral. This equation determines $\mu(x)$ by $dT/d\mu$ in the exclusion zone.

The self-consistent condition eq 2.2 can be written as

$$2\pi(R + x)n(x) = -\int_x^{h^*} \frac{dt(x, x_0)}{dx} 2\pi R\, d\sigma(x_0) \quad (3.6)$$

with $2\pi R\sigma(x_0)$ defined as the number of free ends beyond x_0. Since $n = \mu/\nu$, the above equation yields

$$\frac{\mu}{\nu}(1 + x/R) = \frac{1}{\sqrt{2}a}\int_0^{\mu} \frac{d\mu_0}{(\mu - \mu_0)^{1/2}} \frac{d\sigma}{d\mu_0} \quad (3.7)$$

which upon inversion gives the second integral equation

$$\frac{d\sigma}{d\mu} = \frac{\sqrt{2}a}{\pi}\int_0^{\mu} \frac{d\mu_0}{(\mu - \mu_0)^{1/2}} \frac{d}{d\mu}\left(\frac{\mu}{\nu}[1 + x/R]\right)_{\mu_0} \quad (3.8)$$

Combining eqs 3.5 and 3.8 yields the following equation that determines $dT/d\mu$ in the exclusion zone,

$$\frac{1}{2\pi}\int_Q^P d\mu' \frac{dT}{d\mu'}[K(\mu, \mu') + S(\mu, \mu')] = -\frac{1}{\sqrt{2}a}\frac{R + h}{\sqrt{\mu}} \quad (3.9)$$

with the two kernel functions given by

$$K(\mu, \mu') = \ln\frac{\sqrt{\mu} + \sqrt{\mu'}}{|\sqrt{\mu} - \sqrt{\mu'}|} \quad (3.10)$$

$$S(\mu, \mu') = \frac{1}{2}\left(1 - \frac{\mu'}{\mu}\right)K(\mu, \mu') + \sqrt{\frac{\mu'}{\mu}}$$

Equation 3.9 differs from the corresponding equation for the melt brush by the addition of kernel $S(\mu, \mu')$ which breaks the symmetry under $\mu \leftrightarrow \mu'$. Once $dT/d\mu$ is solved, all the other quantities can be obtained using eqs 3.5 and 3.8.

3.2. Exact Solution in the Strong Curvature Limit. In the strong curvature limit $R \to 0$, $\sigma \to \infty$, and with the number of chains per unit length $\epsilon = 2\pi R\sigma$ fixed, $P/Q \to \infty$. With a change of variables $\mu \to e^t$, $\mu' \to e^s$, eq 3.9 can be cast in the form $\int_0^{\infty} k(s - t)u(s)\, ds = g(t)$. Such an equation can be solved using a technique developed by Wiener and Hopf.[17] We shall omit the detailed derivation and just give the result:

$$\frac{dT}{d\mu} = -\frac{h^*}{\sqrt{2}a}\frac{Q^{3/2}}{\mu^{5/2}(\mu - Q)^{1/2}} \quad (3.11)$$

For large μ, this $dT/d\mu$ scales as μ^{-3} in contrast to the μ^{-2} scaling of the melt.[12] Hereafter we use Q as a unit hence set $Q = 1$. The Q dependence can be recovered by dimensional analysis when necessary.

To obtain the density profile, we first find $dx/d\mu$ through eq 3.5, the result is

$$\frac{dx}{d\mu} = \begin{cases} -\frac{3h^*}{8}g(\mu) & \mu < 1 \\ -\frac{3h^*}{8}\mu^{-5/2}g(1/\mu) & \mu > 1 \end{cases} \quad (3.12)$$

where $g(z)$ is the Gauss' hypergeometric function $F(1/2, 5/2; 3; z)$ defined by[18]

$$g(z) \equiv F(1/2, 5/2; 3; z) = \frac{8}{3\pi}\int_0^1 t^{3/2}(1 - t)^{-1/2}(1 - tz)^{-1/2}\, dt \quad (3.13)$$

Equation 3.12 can be used to compute the density profile $n(x)$. For $x \ll h$, $\mu \gg 1$, $dx/d\mu \sim \mu^{-5/2}$, leading to $n(x) = \mu(x)/\nu \sim x^{-2/3}$, which is a scaling already anticipated by the simple variational calculation. For general x, $n(x)$ is computed by integrating eq 3.12. The result is plotted in Figure 1 as a solid line. We see two distinct regions separated by x_c. $n(x)$ is concave up for $0 < x < x_c$ while concave down for $h > x > x_c$, vanishing smoothly at h. As $x \to x_c$, $dn(x)/dx \to 0$, indicating a vanishing free end density at x_c.

To compute the free end density $\rho(x)$, we use the relation

$$\rho(x) = -\frac{R}{x + R}\frac{d\sigma}{d\mu}\frac{d\mu}{dx} \quad (3.14)$$

In the limit $R \to 0$, $\rho(x)$ is computed using eqs 3.8 and 3.12 and plotted in Figure 1 (solid line). We see that free ends are excluded from the region $0 < x < x_c$. The free end density vanishes at the exclusion zone boundary and at the top of the grafting layer, $\rho(x) \sim (x - x_c)$ as $x \to x_c^+$ while $\rho(x) \sim \sqrt{h^* - x}$ as $x \to h^*$. The exclusion zone height x_c is given by

$$x_c = \int_{\infty}^{1} \frac{dx}{d\mu} d\mu = \frac{4}{3\pi}h^* \approx 0.424h^* \quad (3.15)$$

which is smaller than the corresponding exclusion zone in a cylindrical melt ($x_c = 2h^*/\pi$). So far, we have expressed everything in terms of h^* and Q. It is more transparent to express all the quantities in terms of fundamental variables: the number of monomers N in one chain, and the total number of grafted chains ϵ per unit length of the cylinder. This is accomplished by using the following relations:

$$\int_0^Q 2\pi R\frac{d\sigma}{d\mu} d\mu = \epsilon \quad (3.16)$$

and

$$-\int_Q^P \frac{dT}{d\mu} d\mu = N \quad (3.17)$$

Using eqs 3.16 and 3.17, we find

$$h^* = 0.856098(N^3\nu\epsilon a^2)^{1/4} \quad (3.18)$$

and

$$\mathcal{F}_{\mathrm{min}} = 0.65148\left(\frac{N\epsilon^3\nu}{a^2}\right)^{1/2} \quad (3.19)$$

This free energy is about 5% lower than the one we obtained in section II using the power law stretching ansatz and the general end distribution (eq 2.52).

For comparison, Figure 1 also plots $n(x)$ and $\rho(x)$ from the variation calculation in section II (dotted lines). We see that the variational calculation gives a quite good estimate for the density profile. For the free end distribution, the variational approach overestimates the exclusion zone height and gives a finite nonvanishing density at the zone boundary and the top of the layer. We believe these are artifacts due to the restrictions on the stretching profiles.

Table 1. Free Energy ($\mathcal{F}_{min}$), Layer Height (h^*), and Exclusion Zone Height (r_c) for Planar, Cylindrical, and Spherical Brushes, from the Variational Calculation (Denoted by "Step" and "Smooth" Entries) and the Exact Solution[a]

	$\mathcal{F}_{min}$	h^*	r_c/h^*
	Plane		
step	1	1	1
smooth	0.95	1.26	0
exact	0.89	1.34	0
	Cylinder		
step	1	1	1
smooth	0.99	1.0920	0.79
exact	0.94	1.0924	0.42
	Sphere		
step	1	1	1
smooth	0.9993	1.03	0.94
exact	?	?	?

[a] The results are normalized by the corresponding one in the "step" entry.

IV. Discussion and Future Work

In the previous sections, we have shown that a general variational method can be used to study polymers grafted to curved surfaces. We have applied the method to planar, cylindrical, and spherical brushes. As an alternative method and a check for our variational approach, we solved exactly the self-consistent integral equations for a cylindrical brush in the strong curvature limit. Table 1 lists the calculated layer height, exclusion zone height, and free energy for each case. The "step" entry in the table corresponds to the simplest variational ansatz which assumes identical power law stretching for all the chains. This ansatz gives quite a good estimate for the free energy and the layer height but gives a qualitatively wrong answer for the density profile and free end distribution. As the constraint for the free ends is relaxed, a lower energy configuration is found with right features. This is denoted by the "smooth" entry. For a planar brush, it predicts a parabolic density profile and an end distribution throughout the layer. For both cylindrical and spherical brushes, the "smooth" ansatz predicts an exclusion zone and qualitatively correct density profile. Our results suggest that it is necessary to relax the end constraint in many other problems where the Alexander–de Gennes approximation is used.

A general trend is observed in Table 1: as the solution is improved (from "step" to "smooth" to "exact"), the free energy is lowered, the layer height increased, and the exclusion zone height decreased. This indicates that removal of the constraint on stretching profiles leads to further smearing of the free ends. The exact results for a cylindrical brush show that the smooth ansatz overestimates the exclusion zone height, which we believe is also true for a spherical brush. On the basis of this observation, we expect the exact solution for a star polymer will have $0.42 < r_c/h^* < 0.94$, where the lower bound is given by the exact value for a cylindrical brush, since a sphere is more curved than a cylinder. Another lesson we learn from the cylindrical brush is that the scaling for small r from simple variational calculation is exact, so we expect, for a star polymer, such a scaling should be found for $r \ll h^*$.

Our results are consistent with other information on star and comb polymers. The new information from our work concerns the predicted exclusion zone near the center. For comb polymers, we have noted the agreement between our exact results and the numerical self-consistent calculation of Dan and Tirrell.[19] Their observation of an incipient end-free zone is now supported by our explicit calculation of the asymptotic size of that zone. For the monomer density profile, our analytical solution predicts $n(x) \sim x^{-2/3}$ for $x \ll h^*$, which is consistent with the scaling arguments.[14] However, conflicting powers have been reported in the numerical mean-field study of Dan and Tirrell[19] and the molecular dynamics simulations of Murat and Grest.[20] The authors suggest a falloff as $x^{-1/2}$, more gradual than our $x^{-2/3}$ prediction. We do not regard this as a significant discrepancy. The effective power law observed in these finite-sized systems need not equal the asymptotic power we have derived. Indeed, our analytical solution in Figure 1 shows a more gradual falloff near the exclusion zone boundary. The logarithmic derivative $-(x/n)\, dn/dx$ decreases from $^2/_3$ to 0 as this boundary is approached. If one includes numerical data near this boundary, the measured power is bound to be smaller than the asymptotic one. The molecular dynamics simulation of Murat and Grest[20] verified the expected scaling of the comb thickness with chain density. A narrow exclusion zone appeared only for high line density which was attributed to simple steric packing constraint by the authors. Since the chains in this study were stretched by only a factor less than 4, it appears that the simulation was too far from the strong-stretching limit to see the exclusion zone effect. Several types of comb polymers occur in practice. These typically have short alkane side branches attached to an organic backbone.[21] The main observed impact of the stretching of these side chains is on the induced stiffness in the comb polymer.[22,23] We have seen no evidence regarding the exclusion zone in these polymers. Similar exclusion zones should occur in cylindrical block-copolymer micelles.[24] In addition, the density and pressure at the periphery of such brushes are qualitatively weaker in our exact solution and in our approximations than in the simpler step-function profiles considered previously. This implies that the forces between such brushes in weak contact should be qualitatively smaller than might otherwise be thought. As data about the forces between these cylinders (e.g. by osmotic compressibility) become available, it will be possible to observe these weak forces.

Our results are also of interest for star polymers and spherical micelles. The main experimental observations of these spheres has been the scaling of their size with molecular weight and arm number. Here, as above, our theory has nothing to add to previous scaling theories. However, our theory predicts a monomer density profile and a free end distribution which is qualitatively different. These predictions are also consistent with the numerical calculations of Dan and Tirrell.[19]

Molecular dynamics simulations of stars[25] have shown a concentration of the free ends near the periphery, as in the Daoud–Cotton model. This study did not clearly show our predicted end-containing zone whose thickness should be proportional to the star radius. On the other hand the observed thickness was about as large as that predicted by our best approximation. Thus our approximation is consistent with the simulation results. For chains grafted to a finite sphere, evidence of an exclusion zone was found by Monte-Carlo simulations.[26] Experimental information is available in principle from covalently synthesized star polymers[27] and from spherical micelles of diblock copolymers.[28] Recent scattering experiments[27] have shown evidence for the repulsions between these spheres implicit in our theory. As these experiments are refined, it will become possible to compare the observed repulsion with predictions based on our theory.

Agreement between our results and experiments in good solvents (including simulations) is necessarily limited. This

is because several important features of good solvents have not been incorporated into our model. As noted above, we have ignored the strong local correlations which exclude other chains from the vicinity of a given chain. For such good solvents our models serve as a qualitative guide to the exclusion zone effects. They may only be taken as a quantitative description for marginal solvents in which excluded-volume repulsion is negligible on the scale of the distance between chains.[10]

The mathematics of our exact solution for the cylinder raises several interesting questions. As noted in eqs 3.9 and 3.10 the melt and solvent cases differ only by the addition of a regular kernel S to the singular kernel K in the integral equation. This S is nowhere larger than K; instead K is much larger near its logarithmic singularity. Yet the addition of this small S changes the solution to the equation qualitatively. We believe that this dramatic effect arises from the symmetry of K under exchange of p and p' and the lack of this symmetry in $K + S$. We believe that further analysis of these equations will yield insights about these mutually stretched chains that can result in a more powerful way of treating them.

The variational method we used in this paper can be extended to treat brushes in a good solvent where local Flory swelling of the chains on the scale smaller than interchain distance cannot be ignored.[10] It can also be extended to spheres and cylinders of finite curvature and to other curved surfaces, e.g., undulated surfaces. A large class of problems involves grafted polymers stretched in more than one dimension.[29] So far these problems have been studied only in the Alexander–de Gennes approximation. It will be interesting to see the effect of relaxing the end constraints in these problems.

Acknowledgment. We have benefited from helpful discussions with Scott Milner, Thomas Halsey, and Francisco Solis. This work was supported by the NSF through Grant No. DMR-9208527 and through MRL Grant No. DMR-8819860. H.L. acknowledges partial support by the NSF through PYI Program Grant No. DMR-9057156.

Appendix. Exact Solution for a Spherical Brush in the Alexander–de Gennes Approximation

In this Appendix, we present the exact solution of a spherical brush in which the free ends are excluded from the interior. This is a natural extension of the Alexander–de Gennes approximation used for planar geometry. Others have derived these results[30] though we know of no published derivation. Recall from section 2.2 that for a given h, the solution is determined by the following two equations (eqs 2.31 and 2.30):

$$\frac{v(r)^2}{2a^2} - \frac{vf}{4\pi r^2 v(r)} = C \tag{A.1}$$

and

$$\int_0^h \frac{dr}{v(r)} = N \tag{A.2}$$

where the second equation relates the constant C to h. The equilibrium height h^* should minimize the free energy $\mathcal{F}[h]$. This is equivalent to saying that h^* should be such that the osmotic pressure balances the stretching at the free end. This adds one more constraint which can be used to determine h^*,

$$\frac{vn(h^*)^2}{2} 4\pi h^{*2} = \frac{fv(h^*)}{a^2} \tag{A.3}$$

Using eq A.3 and the relation $n(h^*) = f/(4\pi h^{*2} v(h^*))$, we find

$$v(h^*) = \left(\frac{va^2 f}{8\pi h^{*2}}\right)^{1/3} \tag{A.4}$$

which yields (through eq A.1)

$$C = -\frac{3}{2a^2}\left(\frac{va^2 f}{8\pi h^{*2}}\right)^{2/3} \tag{A.5}$$

Once C is determined, $v(r)$ can be solved from eq A.1. Using dimensionless variables $y(r) = v(r)/v(h^*)$ and $x = r^2/h^{*2}$, eq A.1 becomes

$$y^3 + 3y - 4/x = 0 \tag{A.6}$$

which has a real solution

$$y(x) = \frac{(2 + \sqrt{4 + x^2})^{1/3}}{x^{1/3}} - \frac{x^{1/3}}{(2 + \sqrt{4 + x^2})^{1/3}} \tag{A.7}$$

The equilibrium height h^* is determined by eq A.2,

$$h^* = 0.806857(N^3 a^2 vf)^{1/5} \tag{A.8}$$

The monomer density

$$n(r) = \frac{f}{4\pi r^2 v(r)} = \frac{f}{4\pi r^2 v(h^*) y(r^2/h^{*2})} \tag{A.9}$$

which has a simple scaling $n(r) \sim r^{-4/3}$ for $r \ll h^*$. The total free energy is (according to eq 2.29)

$$\mathcal{F}_{\min} = \int_0^{h^*} dr \left(\frac{fv(r)}{2a^2} + \frac{vf^2}{8\pi r^2 v(r)^2}\right) \tag{A.10}$$

By substituting $v(r)$ into the above expression and using eq A.8, we find

$$\mathcal{F}_{\min} = 1.16369\left(\frac{v^2 f^7 N}{a^6}\right)^{1/5} \tag{A.11}$$

We notice this free energy is about 2% lower than the one we obtained in section 2.2 with the power law assumption of the trajectory and smeared end distribution (eq 2.42). Evidently, better results can be obtained if we start with this exact solution and let the free ends relax. This can be done using a similar ansatz assuming that the stretching profiles of all the chains are proportional to the one given by this exact solution. The calculation will be parallel to that in section 2.2 except that the relation between $n(r)$ and $\rho(r)$ (eq 2.26) takes a complicated form and cannot be inverted explicitly. The results will be similar (i.e., a lower energy configuration will be found with smeared ends and smooth density profile) since the Alexander–de Gennes solution is unstable against smearing of the free ends. We did not carry out such a computation since the purpose of this paper is to demonstrate the power of the variational ansatz through simple examples.

References and Notes

(1) For a review, see e.g.: Milner, S. T. *Science* **1991**, *251*, 905. Halperin, A.; Tirrell, M.; Lodge, T. P. *Adv. Polym. Sci.* **1992**, *100*, 31.
(2) de Gennes, P. G. *J. Phys. (Paris)* **1976**, *37*, 1443. de Gennes, P. G. *Macromolecules* **1980**, *13*, 1069.
(3) Alexander, S. *J. Phys. (Paris)* **1977**, *38*, 977.
(4) Helfand, H. E.; Wasserman, Z. R. *Macromolecules* **1978**, *11*, 960.

(5) Scheutjens, J. M. H. M.; Fleer, G. J. *J. Phys. Chem.* **1979**, *83*, 1619.
(6) Ben-Shaul, A.; Szleifer, I.; Gelbart, W. M. *J. Chem. Phys.* **1985**, *83*, 3597.
(7) Viovy, J. L.; Gelbart, W. M.; BenShaul, A. *J. Chem. Phys.* **1987**, *87*, 4114.
(8) Noolandi, J.; Hong, K. M. *Macromolecules* **1982**, *15*, 482.
(9) Semenov, A. N. *Sov. Phys. JETP* **1985**, *61*, 733; *Zh. Eksp. Teor. Fiz.* **1985**, *88*, 1242.
(10) Milner, S. T.; Witten, T. A.; Cates, M. E. *Macromolecules* **1988**, *21*, 2610.
(11) Zhulina, E. B.; Pryamitsyn, V. A.; Borisov, O. V. *Vysokomol. Soedin., Ser. A* **1989**, *31*, 185 and references therein.
(12) Ball, R. C.; Marko, J. F.; Milner, S. T.; Witten, T. A. *Macromolecules* **1991**, *24*, 693.
(13) Daoud, M.; Cotton, J. P. *J. Phys. (Paris)* **1982**, *43*, 531.
(14) Birshtein, T. M.; Borisov, O. V.; Zhulina, E. B.; Khokhlov, A. R.; Yurasova, T. A. *Polym. Sci. USSR* **1987**, *29*, 1293.
(15) Edwards, S. F. *Proc. Phys. Soc. (London)*, **1965**, *93*, 605.
(16) More rigorously, α is solved using eq 2.6 for a given h, and the equilibrium height h^* is obtained by minimizing the free energy with respect to h. The resulting h^* satisfies the condition $n(h^*) = 0$. This is a general result not restricted to planar geometry as demonstrated in sections 2.2 and 2.3.
(17) Wiener, N.; Hopf, E. *S.B. Preuss. Akad. Wiss.* **1931**, 696.
(18) See e.g.: *Handbook of Mathematical Functions*; Abramowitz, M., Stegun, I., Eds.; Dover, 1965.
(19) Dan, N.; Tirrell, M. *Macromolecules* **1992**, *25*, 2890.
(20) Murat, M.; Grest, G. S. *Macromolecules* **1991**, *24*, 704.
(21) Lin, J. K.; Yuki, Y.; Kunisada, H. *Polym. J.* **1992**, *22*, 92 and references therein.
(22) Fredrickson, G. H. *Macromolecules* **1993**, *26*, 2825.
(23) Cao, Y.; Smith, P. *Polym. Commun.*, submitted for publication. Cao, Y.; Smith, P.; Heeger, A. J. *Synth. Met.* **1992**, *48*, 91.
(24) Winey, K. I.; Thomas, E. L.; Fetters, L. J. *J. Chem. Phys.* **1991**, *95*, 12.
(25) Grest, G. S.; Kremer, K.; Milner, S. T.; Witten, T. A. *Macromolecules* **1989**, *22*, 1904.
(26) Toral, R.; Chakrabarti, A. Preprint.
(27) Dozier, W. D.; Huang, J. S.; Fetters, L. J. *Macromolecules* **1991**, *24*, 2810.
(28) Tuzar, Z.; Kratochvil, P. *Surface Colloid Sci.* **1993**, *15*, 1 and references therein.
(29) E.g.: Fredrickson, G. H.; Ajdari, A.; Leibler, L.; Carton, J. P. *Macromolecules* **1992**, *25*, 2882. Fredrickson, G. H. Preprint.
(30) E.g.: Milner, S. T. Private communication.